www.czasopisma.pan.pl PAN www.journals.pan.pl
Opto-Electronics Review 25 (2017) 209–214

Contents lists available at ScienceDirect

Opto-Electronics Review

journal homepage: http://www.journals.elsevier.com/opto-electronics review

Luminescence of II–VI and III–V nanostructures☆

K.D. Mynbaev[a,b,*], A.V. Shilyaev[a], A.A. Semakova[a,b], E.V. Bykhanova[a,b], N.L. Bazhenov[a]

[a] *Ioffe Institute, Saint–Petersburg, 194021, Russia*
[b] *ITMO University, Saint–Petersburg, 197101, Russia*

ARTICLE INFO

Article history:
Received 3 November 2016
Accepted 4 March 2017
Available online 24 July 2017

Keywords:
mid-infrared range
luminescence
nanostructures

ABSTRACT

Photoluminescence of HgCdTe epitaxial films and nanostructures and electroluminescence of InAs(Sb,P) light-emitting diode (LED) nanoheterostructures were studied. For HgCdTe-based structures, the presence of compositional fluctuations, which localized charge carriers, was established. A model, which described the effect of the fluctuations on the rate of the radiative recombination, the shape of luminescence spectra and the position of their peaks, was shown to describe experimental photoluminescence data quite reasonably. For InAs(Sb,P) LED nanoheterostructures, at low temperatures (4.2–100 K) stimulated emission was observed. This effect disappeared with the temperature increasing due to the resonant 'switch-on' of the Auger process involving transition of a hole to the spin-orbit-splitted band. Influence of other Auger processes on the emissive properties of the nanoheterostructures was also observed. Prospects of employing II–VI and III–V nanostructures in light-emitting devices operating in the mid-infrared part of the spectrum are discussed.

1. Introduction

It is known that characteristic absorption bands of many important chemicals (CH_4, CO_2, NO_2, H_2S, CO, etc.) are located in the mid-infrared wavelength range (MWIR, wavelengths λ 2–6 μm) [1]. Sensors of these chemicals are required by industry, for environmental control purposes and in medicine. The most promising are MWIR sensors based on light-emitting diodes and semiconductor photodetectors. It is useful to fabricate light emitters and photodetectors on the basis of the same materials, as it greatly simplifies manufacturing process.

To enhance the efficiency of optoelectronic devices, it is important to understand and control processes which take place under absorption and/or emission of light in real structures. For that task, it is useful to study their operation not only at working temperatures, but also at low temperatures. In this case, effects could be observed that allow for more detailed identification of the mechanisms of physical processes. Within the frames of such approach, we have studied luminescence of epitaxial films and nanostructures based on II–VI (HgCdTe) and III–V (InAs(Sb,P)) semiconductors in a wide temperature range, from 4.2 K up to 300 K. The energy gap of the studied materials corresponded to the MWIR range.

2. Details of experimental technique

Photoluminescence (PL) of HgCdTe-based structures and electroluminescence (EL) of InAs(Sb,P)-based structures were studied. The PL signal was excited by a semiconductor laser with λ = 1.03 μm, which operated in a pulsed mode (frequency 1 kHz, pulse duration 1 μs). For signal detection, a cooled InSb photodiode and a boxcarintegrator were used. EL experiments were conducted in a similar pulsed excitation mode with the same detector.

3. Photoluminescence of II–VI structures

3.1. Experimental data

HgCdTe-based epitaxial films were grown with Liquid-Phase Epitaxy (LPE) and Molecular-Beam Epitaxy (MBE) and had thickness of 5 to 9 μm. HgCdTe-based nanostructures were grown with MBE and represented structures with potential wells, whose width did not provide size quantization (for $Hg_{1-x}Cd_xTe$ chemical compositions x considered, >100 nm). The values of x were determined with optical transmission studies. To relate the energy gap E_g to x and temperature T, the $E_g(x,T)$ dependence from Ref. [2] was used.

☆ This article is an expanded version of a scientific report presented at the International Conference on Semiconductor Nanostructures for Optoelectronics and Biosensors 2016 ICSeNOB2016, May 22–25, 2016, Rzeszow, Poland.

* Corresponding author at: Polytechnicheskaya 26, Saint-Petersburg, 194021, Russia.
E-mail address: mynkad@mail.ioffe.ru (K.D. Mynbaev).

http://dx.doi.org/10.1016/j.opelre.2017.06.005
1230-3402/

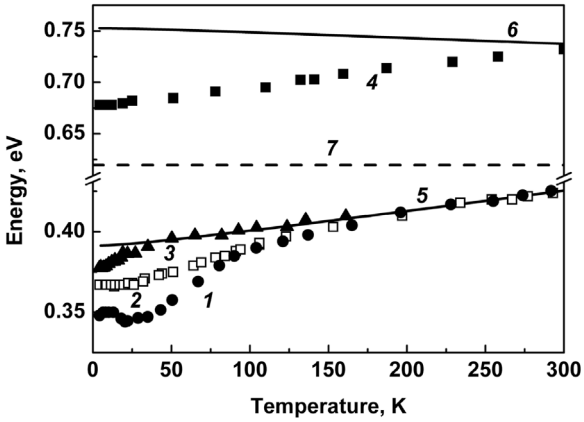

Fig. 1. Experimental temperature dependences of PL peak position for three HgCdTe-based structures with $x = 0.38$ (MBE HgCdTe/GaAs (*1*), MBE HgCdTe/Si (*2*) and LPE HgCdTe/CdTe (*3*)), and MBE-grown HgCdTe/GaAs with $x = 0.57$ (*4*). Lines show calculated dependences $E_g(T)$ for HgCdTe with $x = 0.38$ (*5*), $x = 0.57$ (*6*) and, for a reference, $x = 0.50$ (*7*).

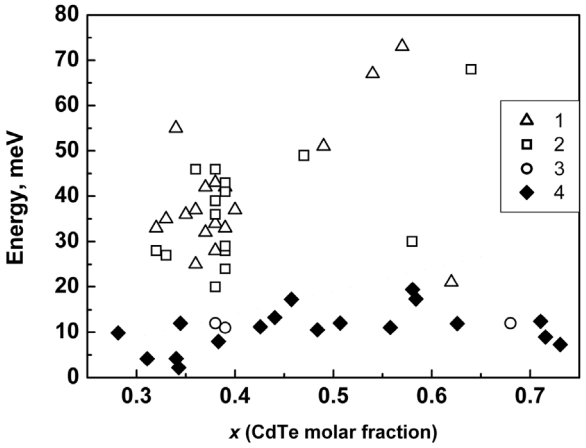

Fig. 2. Experimental dependence of «exciton localization energy» according to PL data on the composition of HgCdTe alloy: MBE HgCdTe/GaAs (*1*), MBE HgCdTe/Si (*2*) and LPE HgCdTe/CdTe (*3*), and similar data obtained on THM and LPE HgCdTe and presented in Refs. [12,13] (*4*).

HgCdTe alloy is the material of choice for fabricating infrared photodetectors, but it has been also considered as a prospective material for light emitters, typically with optical excitation [3,4]. This makes luminescence studies of HgCdTe-based structures quite important. Most of our original experimental data on PL studies of HgCdTe-based structures were presented elsewhere [5–9]. Fig. 1 shows, as an example, a temperature dependence of the position (in energy units, eV) of a 'band-to-band' (excitonic) PL peak E_{PL} for three HgCdTe-based structures with $x = 0.38$ (grown with MBE on GaAs and Si substrates and with LPE on CdTe substrate), and that for an MBE-grown structure (GaAs substrate) with $x = 0.57$. Calculated $E_g(x,T)$ dependences for HgCdTe with corresponding x values are also shown. As can be seen, at low temperatures a considerable difference between E_{PL} and calculated E_g is observed, but with temperature increasing this difference diminishes. Also, for the sample with $x = 0.57$ we observe different slope sign for experimental $E_{PL}(T)$ and calculated $E_g(T)$ dependence. For HgCdTe-based structures, this is typically explained by the fact that 'band-to-band' PL at low temperatures is due to recombination of excitons localized at compositional fluctuations [5–13]. Then, the difference Δ between E_{PL} and E_g should somehow define exciton localization energy and, therefore, is indicative of the fluctuation scale [10–13]. (The latter may be also characterized by the full-width at half-maximum (FWHM) of the excitonic PL line). Following this idea, on the basis of the data presented in Fig. 1 we can state that the structure grown with LPE has the lowest fluctuation amplitude, while the sample grown with MBE on GaAs substrate has the largest amplitude, as all these samples have the same $x = 0.38$.

Fig. 2 summarizes the data on Δ *vs.* alloy composition from our experiments. Also, presented are data on exciton localization energy available in the literature ([12,13]) and obtained on HgCdTe crystals grown with Travelling Heater Method (THM) and on LPE-grown films. Due to the use of different models for estimating the exciton localization energy, different $E_g(x,T)$ dependences, etc., quantitative comparison of our data with those from Refs. [12,13] would not be valid. However, we can make a qualitative conclusion that structures grown with THM and LPE have much smaller compositional fluctuations than those grown with MBE. Let us also note that, when speaking of stochastic character of fluctuations, the maximum fluctuation amplitude and, therefore, the maximum exciton localization energy, should be observed for the material with $x = 0.50$ [12–14]. THM- and LPE-grown samples generally obey this rule while MBE–grown structures show the tendency of Δ increasing with x up to $x \sim 0.63$. All these data witness to the fact

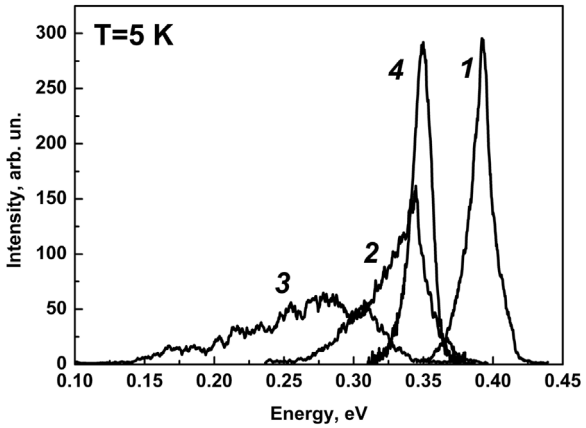

Fig. 3. PL spectra calculated within the frames of the model for HgCdTe with $x = 0.38$ at $T = 5$ K with various fluctuation amplitudes: 16 meV (*1*), 28 meV (*2*), and 70 meV (*3*) and experimental PL spectrum of MBE/GaAs HgCdTe with the same x (*4*). Intensities of the calculated spectra cannot be compared to that of the experimental one.

that alloy disorder in MBE-grown MCT is not of a stochastic nature but is rather caused by the specifics of the growth technology. This does not come as a surprise, as for some semiconductor alloys, e.g., InGaN, such 'technological' disorder has been studied in detail [15], and for AlGaN alloys it is now introduced intentionally, as localization of exctions on compositional fluctuations has proven to increase quantum yield in optoelectronic devices [16].

3.2. Discussion

To interpret the experimental data obtained, we developed a model which described the effect of fluctuations on the rate of radiative recombination, the shape of PL spectra and the position of their peaks. A hybrid model was developed, in which the state of each carrier was described with a Gaussian-type wave packet, which contained co-ordinates and impulses of the particle as parameters. The details of the model were presented elsewhere [17].

Fig. 3 shows PL spectra of HgCdTe sample with $x = 0.38$ generated with the use of the model for three fluctuation amplitudes (the spectra were subjected to 5-point averaging). Each calculated spectrum contains information on 10,000 radiative transitions. It is seen that with the fluctuation amplitude increasing, the peak of the spectrum is red-shifting (compare curves *1* and *2*), as the increase in

the potential depth leads to the decrease in local value of energy gap and, therefore, decreases the energy of the emitted photon. Also, it is seen that with the fluctuation amplitude increasing, the FWHM of the spectrum increases. This is explained by the increase in the scatter of local energy minima that contribute to the PL signal. The integral PL intensity remains constant.

Further increase in the fluctuation amplitude significantly distorts the shape of the spectrum (curve *3* in Fig. 3). The long-wavelength part of the spectrum now shows 'extra peaks', which are due to the emission from local areas that contain fluctuations with very large depth. Localization of carriers in such areas leads to appearance of a number of separate emission peaks. This effect has been demonstrated experimentally for III-nitride alloys [18]. The short-wavelength part of the spectra both in the model and in the experiment retains the Gaussian-like shape irrespective of the fluctuation amplitude.

As follows from Fig. 3, for HgCdTe with $x = 0.38$ the given experimental spectrum for MBE-grown material (GaAs substrate) in terms of FWHM appeared to be closest to the modeled spectrum with fluctuation amplitude 16 meV (curves *4* and *1*, respectively). At the same time, in terms of Δ, the experimental spectrum was closer to the modeled one with fluctuation amplitude 28 meV (curve *2*). 16 to 28 meV amplitude range constitutes 4 to 7% of the energy gap value (~390 meV at $T = 5$ K). The actual experimental Δ values for MBE-grown HgCdTe with $x = 0.38$ vary from 20 to 45 meV (see Fig. 2). We can conclude that qualitatively the model describes the effect of compositional fluctuations on the radiative recombination in HgCdTe-based structures quite reasonably. The future development of the model should consider the transformation of the shape of the PL spectra of MBE-grown HgCdTe with temperature [7], as well as the very fact of the observation of PL from a narrow-gap semiconductor at high (up to 300 K) temperatures. The latter currently contradicts the results of the latest calculations of radiative and non-radiative carrier lifetimes in the material, which, for example, predict the dominance of Auger recombination in HgCdTe with $x = 0.3$ at temperatures higher than $T = 230$ K [19]. On the other hand, strong PL of HgCdTe-based MBE-grown structures at 300 K opens prospects for employing this material in light emitters in MWIR range, where III-V-based structures experience problems due to specific electronic structure, as will be discussed in the next section.

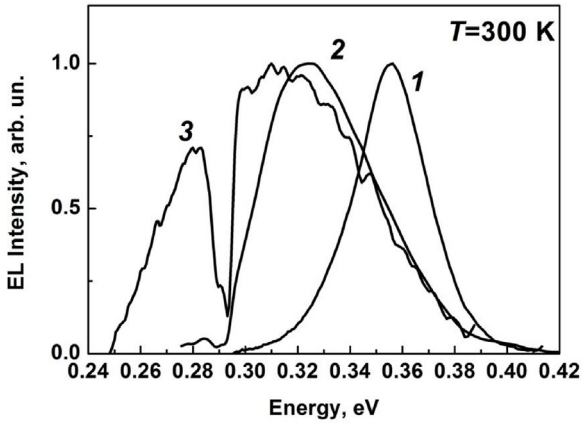

Fig. 4. Normalized EL spectra of heterostructures of type A (InAs active layer) (curve *1*), type B (InAsSb active layer) (curve *2*) and type C (MQWs in the active layer) (curve *3*) at $T = 300$ K. A dip near 0.29 eV is due to absorption by the atmosphere.

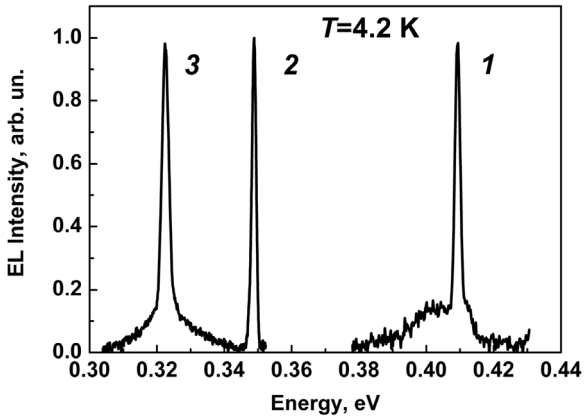

Fig. 5. Normalized EL spectra of heterostructures of type A (InAs active layer, $I = 0.6$ A) (curve *1*), type B ($InAs_{0.93}Sb_{0.07}$ active layer, $I = 0.6$ A) (curve *2*) and type C (MQWs in the active layer, $I = 1.4$ A) (curve *3*) at $T = 4.2$ K.

4. Electroluminescence of III–V structures

4.1. Experimental data

InAs(Sb,P) heterostructures were grown with metal-organic vapour-phase epitaxy, the growth technique was described elsewhere [20]. Fig. 4 shows typical normalized EL spectra of the three types of studied heterostructures at $T = 300$ K. In heterostructures of type A, the active region with thickness 1–2 μm was made of InAs. In heterostructures of type B, the active region was made of InAsSb with an InSb molar fraction of 0.07. In heterostructures of type C, the active region was constituted by multiple (108 pcs) quantum wells (MQW) InAsSb/InAs (4 nm/10 nm) with InSb molar fraction in the well of 0.12. All the structures were grown on highly doped (electron concentration at 77 K $n_{77} = 2 \times 10^{18}$ cm^{-3}) *n*-type InAs substrates, and on top of the active layer a wide-bandgap InAsSbP *p*-type barrier layer was grown. Electron concentration in the active layer was $n_{77} = (8–20) \times 10^{15}$ cm^{-3}.

The spectra presented in Fig. 4 appeared to be typical of MWIR LEDs with FWHMs being ~35 meV for the structure of type A, ~50 meV for the structure of type B and ~80 meV for the structure of type C.

Fig. 5 shows normalized EL spectra of the three types of studied heterostructures at $T = 4.2$ K and various driving currents *I*. As can be seen, these spectra differ greatly in shape and width from those recorded at 300 K. For example, for the structure of type A, at the high-energy side of the wide emission band (with FWHM 20 meV, which would correspond to the narrowing of the initial EL bandwidth with the temperature decreasing), there appeared a second narrow line with FWHM of 2 meV. Our study of the dependences of these bands on *I* showed that with the latter increasing from 0.1 up to 0.6 A, the intensity of the wide band was increasing insignificantly, while that of the narrow band increased substantially.

For the structures of type B at the temperatures close to that of liquid helium, we also observed very narrow peaks. With increasing of the current, the integral EL intensity was increasing linearly, while the peak maximum was blue-shifting, possibly reflecting the filling of the conduction band and lifting of the Fermi quasi-level for electrons. PL spectra of the structures of type B at $T = 77$ K previously demonstrated a clearly defined modal structure [21].

For the structures of type C with the active layer made of InAsSb/InAs MQWs, at temperatures $T < 50$ K we also observed very narrow peaks. However, a considerably larger driving current was required to achieve this effect as compared to the structures of types A and B.

With temperature increasing, for all the structures we observed a sharp transition from narrow EL peaks to broad ones. The exact transition point depended on the type of structure and the driving current. Fig. 6 shows the energy of the EL peaks E_{EL} vs. temperature for a structure of type A. All the spectra were recorded at the

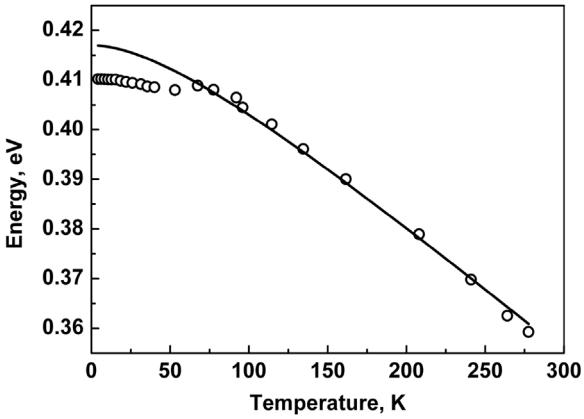

Fig. 6. The experimental dependence of the energy position of EL peak on the temperature for a structure of type A (symbols) and calculated $E_g(T)$ dependence for the active layer made of InAs (straight curve).

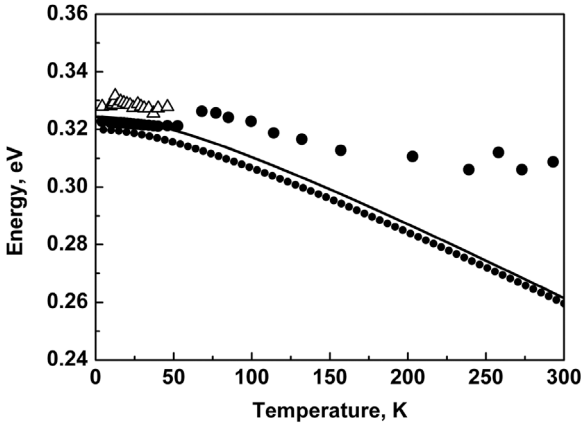

Fig. 7. The dependence of the position of EL peaks for a structure of type C (MQW active region) (large symbols), calculated E_g of $InAs_{0.93}Sb_{0.07}$ — the material of the QWs (straight line), and calculated energy of optical transitions E_{opt} (line + small symbols).

same driving current $I = 0.6$ A (for this sample, at this current at low temperatures only narrow EL peak was observed). It is seen that at $T \geq 70$ K the emission energy corresponds to the value of the energy gap E_g of the active layer calculated in accordance with the data presented in Ref. [22]. At lower temperatures, when the peak of EL was narrow, the energy of the peak was lower than the E_g value.

Similar dependences of E_{EL} on the temperature were observed for structures of type B. In this case, however, at higher temperatures (typically T > 100 K) E_{EL} values were larger than those of calculated E_g by ~20 meV. As the electron effective mass in the alloys was smaller than that in InAs, this could be easily explained by the filling of the conduction band and lifting of the Fermi quasi-level for electrons according to the Burstein-Moss effect. At T < 100 K, values of E_{EL} were close to calculated E_g.

Fig. 7 shows E_{EL} *vs.* temperature for a structure of type C, where both narrow and broad EL peaks were present in the spectra recorded at low temperatures. Calculations of the electronic structure of MQWs region with an account for fractional band offsets in such materials as proposed in Ref. [23] showed that there we dealt with a set of type II heterojunctions, size quantization being achieved for holes in InAsSb and for electrons in InAs. So, optical transitions most probably occur between these quantization levels. The energy of the first quantization level for holes E_h and electrons E_e was calculated, and optical bandgap value $E_{opt} = E_g(InAsSb) + E_h(InAsSb) + E_e(InAs) - \Delta E_c$ where ΔE_c is the conduction band offset. This value appeared to be close to that of the E_g of the material in quantum well. As can be seen in Fig. 7, at low temperatures the E_{EL} of a wide emission band followed the E_g, while narrow EL peak had the energy higher than the E_g value. The energy of both peaks exceeded that of the expected optical bandgap E_{opt}.

Table 1
Δ_{SO} and energy of transition from stimulated to spontaneous emission in the studied structures.

Structure type/Active layer	Calculated Δ_{SO}, eV	'Transition' energy, eV from experiment
A/InAs	0.37–0.41	~0.41
B/InAsSb	0.33–0.37	~0.34
C/MQW	0.30–0.34	~0.32

With temperature increasing, the narrow peak disappeared. In a short temperature range (60–150 K in Fig. 7), E_{EL} generally followed the temperature dependence of E_g of the material of QWs (or calculated E_{opt}), exceeding the former by 15 meV. However, at $T > 150$ K E_{EL} became virtually independent of the temperature. This behaviour, among other reasons, can be attributed to the fact that in this multi-well structure one could expect formation of a certain band structure consisting of two energy bands generated by the energy levels in the wells. Such structure may cause a very different temperature dependence of its bandgap but the problem needs a further study.

4.2. Discussion

The analysis of the results obtained shows that at low temperatures (4.2–100 K), in the studied InAs(Sb,P) structures, conditions for stimulated emission held true. Speaking of LED structures with the active layer made of InAs, a similar effect was first reported on in Ref. [24] (note that there, in contrast to the present work, double heterostructures were studied). Stimulated emission from structures with InAsSb-based active layer so far has been observed only in specially designed laser structures: in particular, one can mention strip-waveguide lasers based on double heterostructures with high symmetrical barriers [25–27]. In our case, resonators were not fabricated, nor were the cleft edges of the LED chips mirror-like. The inter-mode spacing in the EL spectra of 6 nm [21] allowed, using a simple method described in Ref. [27], for assessing the length of the resonator as 280 μm. This value appeared to be much closer to the thickness of the LED chip (~300 μm) rather than to the distance between the cleft edges of the chip (380 μm). Also, it appeared that EL signal in the stimulated emission mode coming from the surface of the chips was much stronger than that collected from the chip edges. Thus, we concluded that in our structures optical resonator was formed normal to the growth plane, most probably, between the surface of the chip with gold Ohmic contact and the substrate, which was polished chemically in the process of making LEDs in accordance with the requirements of the 'flip-chip' technology.

The experimental data showed that transition from stimulated emission to spontaneous one occurred at different temperatures (50–100 K) for different structures. Table 1 shows that actually this transition was not related to a particular temperature, but rather, to the energy of the bandgap: the transition occurred when the energy of the 'effective' bandgap coincided with the energy of spin-orbit splitting Δ_{SO} in the material of the active layer (Δ_{SO} was calculated on the basis of the data from Ref. [22]). Obviously, with temperature increasing and 'effective' E_g decreasing, we observed a resonant 'switch-on' of the CHHS Auger process, when the energy of recombining electron-hole pair was transferred to a hole transitioning to the spin-orbit-splitted band. This effect is well known for narrow-gap III–V semiconductors (see, e.g., [28–30]) and this contrasts them to II–VI materials, and in particular, to HgCdTe,

where $\Delta_{SO} \sim 1$ eV and does not affect properties of devices operating in the MWIR range [31]. With further temperature increasing and E_g decreasing, the resonance $E_g = \Delta_{SO}$ disappeared, but still we observed spontaneous emission. This was obviously due to the influence of Auger processes of other types, which suppressed amplification. Likely, the dominating process was that with the participation of two electrons and a heavy hole with excitation of electron in more energetic state (CHCC). Let us note that the effect of the CHCC Auger process was observed at low temperatures, too. Namely, for the structures of type B at low temperatures, when the emission was still stimulated, we measured power-current characteristics and plotted the temperature dependence of the threshold current for stimulated emission (not shown). From 70 up to 130 K this dependence was exponential, which indicated contribution of Auger processes [32].

Regarding MQW structures, the behaviour of $E_{EL}(T)$ dependence might also indicate that in these LED heterostructures at different temperatures carrier recombination occurs at the different regions of the structure. This effect definitely needs further study, but from the practical point of view, a LED with the wavelength not dependent on the temperature in such a wide temperature range looks quite promising. Generally, the results obtained showed that the efficiency of MWIR LEDs based on InAs(Sb,P) could be increased via suppression of Auger recombination and improvement of carrier confinement in the active region.

5. Conclusions

Photoluminescence of epitaxial films and nanostructures based on narrow-gap HgCdTe alloys was studied experimentally. The presence of nano-sized compositional fluctuations, which localized charge carriers, was established. A model, which describes the effect of the fluctuations on the rate of the radiative recombination, the shape of PL spectra and the position of their peaks, demonstrates how carrier localization shows off in the specific features of the luminescence spectra, and allows for qualitatively relating these features to the actual scale of the fluctuations. From the practical point of view, the presence of fluctuations, their scale, and the range of this scale, which cannot be predicted at the stage of the growth, makes MBE-grown HgCdTe not quite viable for fabrication of light emitters working at low temperatures, even at 77 K. On the other hand, unexpectedly strong luminescence of this material at temperatures close to 300 K allows for suggesting that the idea of HgCdTe-based light emitters may be re-visited.

Electroluminescence of light-emitting InAs(Sb,P) nanostructures was also studied. At low temperatures (4.2–100 K), stimulated emission from the structures was observed. This effect, however, disappeared with the temperature increasing due to the resonant 'switch-on' of the CHHS Auger process, and could not be observed further due to the influence of other Auger processes. The effect of the Auger recombination was established for low temperatures, as well. Despite this, it looks that InAs(Sb,P) nanostructures are promising in respect to the fabrication of the vertical-emitting MWIR lasers, as even under the strong influence of Auger recombination it appears to be possible to get stimulation emission with minimum requirements for optical resonators. Suppressing Auger recombination and improving carrier confinement in narrow-gap III–V structures remain very topical tasks.

Acknowledgements

The authors should like to thank their colleagues who provided structures for this research, in particular, S.A. Dvoretsky, V.S. Varavin, M.V. Yakushev and N.N. Mikhailov (HgCdTe samples grown with MBE) and N.D. Stoyanov, S.S. Kizhaev, S.S. Molchanov, A.P. Astakhova, and A.V. Chernyaev (InAs(Sb,P) LEDs). The work at ITMO University got support from Russian Science Foundation, Research project No. 14-29-00086.

References

[1] A. Krier (Ed.), Mid-Infrared Semiconductor Optoelectronics. Springer Series in Optical Sciences, vol. 118, Springer, Berlin, 2006.
[2] C.R. Becker, V. Latussek, A. Pfeuffer-Jeschke, G. Landwehr, L.W. Molenkamp, Band structure and its temperature dependence for type-III HgTe/$Hg_{1-x}Cd_xTe$ superlattices and their semimetal constituent, Phys. Rev. B 62 (2000) 10353–10363.
[3] J.P. Zanatta, F. Noël, P. Ballet, N. Hdadach, A. Million, G. Destefanis, E. Mottin, C. Kopp, E. Picard, E. Hadji, HgCdTe molecular beam epitaxy material for microcavity light emitters: application to gas detection in the 2-6 μm range, J. Electron. Mater. 32 (2003) 602–607.
[4] C.R. Tonheim, A.S. Sudbø, E. Selvig, R. Haakenaasen, Enhancement of light emission from Hg-Cd-Te due to surface patterning, IEEE Photon. Technol. Lett. 23 (2011) 36–38.
[5] V.I. Ivanov-Omskii, N.L. Bazhenov, K.D. Mynbaev, Effect of alloy disorder on photoluminescence in HgCdTe, Phys. Status Solidi B 246 (2009) 1858–1869.
[6] K.D. Mynbaev, N.L. Bazhenov, V.I. Ivanov-Omskii, N.N. Mikhailov, M.V. Yakushev, A.V. Sorochkin, S.A. Dvoretsky, V.S. Varavin, Yu. G. Sidorov, Photoluminescence of $Hg_{1-x}Cd_xTe$ based heterostructures grown by molecular–beam epitaxy, Semiconductors 45 (2011) 872–879.
[7] K.D. Mynbaev, N.L. Bazhenov, A.V. Shilyaev, S.A. Dvoretsky, N.N. Mikhailov, M.V. Yakushev, V.G. Remesnik, V.S. Varavin, High–temperature photoluminescence of CdHgTe solid solutions grown by molecular–beam epitaxy, Tech. Phys. 58 (2013) 1536–1539.
[8] A.I. Izhnin, A.I. Izhnin, K.D. Mynbaev, N.L. Bazhenov, A.V. Shilyaev, N.N. Mikhailov, V.S. Varavin, S.A. Dvoretsky, O.I. Fitsych, A.V. Voitsekhovsky, Photoluminescence of HgCdTe nanostructures grown by molecular beam epitaxy on GaAs, Opto-Electron. Rev. 21 (2013) 390–394.
[9] K.D. Mynbaev, A.V. Shilyaev, N.L. Bazhenov, I.I. Izhnin, A.I. Izhnin, N.N. Mikhailov, V.S. Varavin, S.A. Dvoretsky, Acceptor states in heteroepitaxial CdHgTe films grown by molecular–beam epitaxy, Semiconductors 49 (2015) 367–372.
[10] J.W. Tomm, K.H. Herrmann, A.E. Yunovich, Infrared photoluminescence in narrow-gap semiconductors, Phys. Status Solidi A 122 (1990) 11–42.
[11] F. Fuchs, P. Koidl, Carrier localization in low-bandgap $Hg_{1-x}Cd_xTe$ crystals, studied by photoluminescence, Semicond. Sci. Technol. 6 (1991) C71–C75.
[12] A. Lusson, F. Fuchs, Y. Marfaing, Systematic photoluminescence study of $Cd_xHg_{1-x}Te$ alloys in a wide composition range, J. Cryst. Growth 101 (1990) 673–677.
[13] P. Gille, K.H. Herrmann, N. Puhlmann, M. Schenk, J.W. Tomm, L. Werner, E_g versus x relation from photoluminescence and electron microprobe investigations in p-type $Hg_{1-x}Cd_xTe$ ($0.35 \le x \le 0.7$), J. Cryst. Growth 86 (1988) 593–598.
[14] M.M. Kraus, C.R. Becker, S. Scholl, Y.S. Wu, S. Yuan, G. Landwehr, Infrared photoluminescence on molecular beam epitaxy grown $Hg_{1-x}Cd_xTe$ layers, Semicond. Sci. Technol. 8 (1993) S62–S65.
[15] G.B. Stringfellow, Microstructures produced during the epitaxial growth of InGaN alloys, J. Cryst. Growth 312 (2010) 735–749.
[16] Y. Liao, C. Kao, C. Thomidis, A. Moldawer, J. Woodward, D. Bhattarai, T.D. Moustakas, Recent progress of efficient deep UV-LEDs by plasma-assisted molecular beam epitaxy, Phys. Status Solidi C 9 (2012) 798–801.
[17] A.V. Shilyaev, A.A. Greshnov, N.L. Bazhenov, K.D. Mynbaev, Modeling recombination processes in solid solutions with large-scale composition fluctuations, Mater. Phys. Mech. 18 (2013) 171–178.
[18] S. De, A. Layek, A. Raja, A. Kadir, M.R. Gokhale, A. Bhattacharya, S. Dhar, A. Chowdhury, Two distinct origins of highly localized luminescent centers within InGaN/GaN quantum-well light-emitting diodes, Adv. Funct. Mater. 21 (2011) 3828–3835.
[19] K.D. Mynbaev, A.V. Shilyaev, N.L. Bazhenov, A.I. Izhnin, I.I. Izhnin, A.V. Voitsekhovskii, N.N. Mikhailov, V.S. Varavin, S.A. Dvoretsky, Light emission from CdHgTe–based nanostructures, Mater. Phys. Mech. 21 (2014) 112–118.
[20] M. Sopanen, T. Koljonen, H. Lipsanen, T. Tuomi, Growth of GaInAsSb using tertiarybutylarsine as arsenic source, J. Cryst. Growth 145 (1994) 492–497.
[21] N.K. Zhumashev, K.D. Mynbaev, N.L. Bazhenov, N.D. Stoyanov, S.S. Kizhaev, T.I. Gurina, A.P. Astakhova, A.V. Tchernyaev, S.S. Molchanov, H. Lipsanen, Kh.M. Salikhov, V.E. Bougrov, Spectral characteristics of mid-infrared light-emitting diodes based on InAs(Sb,P), Sci. Technol. J. Inform. Technol. Mech. Opt. 16 (2016) 76–84.
[22] I. Vurgaftman, J.R. Meyer, L.R. Ram-Mohan, Band parameters for III-V compound semiconductors and their alloys, J. Appl. Phys. 89 (2001) 5815–5875.
[23] E.H. Steenbergen, O.O. Cellek, D. Lubyshev, Y. Qiub, J.M. Fastenau, A.W.K. Liub, Y.-H. Zhang, Study of the valence band offsets between InAs and $InAs_{1-x}Sb_x$ alloys, Proc. SPIE 8268 (2012) 82680K.
[24] N. Matveev, N. Zotova, S. Il'inskaya, M. Karandashev, M. Remennyi, N. Stus', Spontaneous and stimulated emission in InAs LEDs with cavity formed by gold anode and semiconductor/air interface, Phys. Status Solidi C 2 (2005) 927–930.

[25] B. Lane, M. Razeghi, High-power electrically injected mid-infrared interband lasers grown by LP-MOCVD, J. Cryst. Growth 221 (2000) 679–682.
[26] A.P. Astakhova, T.V. Bez'yazychnaya, L.I. Burov, A.S. Gorbatsevich, A.G. Ryabtsev, G.I. Ryabtsev, M.A. Shchemelev, Yu.P. Yakovlev, Optical parameters of diode lasers based on an InAsSb/InAsSbP heterostructures, Semiconductors 42 (2008) 228–231.
[27] E.A. Grebenshchikova, N.V. Zotova, S.S. Kizhaev, S.S. Molchanov, Yu.P. Yakovlev, InAs/InAsSbP light-emitting structures grown by gas-phase epitaxy, Tech. Phys. 46 (2001) 1125–1127.
[28] J.R. Lindle, J.R. Meyer, C.A. Hoffman, F.J. Bartoli, G.W. Turner, H.K. Choi, Auger lifetime in InAs, InAsSb, and InAsSb-InAlAsSb quantum wells, Appl. Phys. Lett. 67 (1995) 3153–3155.
[29] P. Adamiec, R. Bohdan, A. Bercha, F. Dybala, W. Trzeciakowski, Y. Rouillard, A. Joullié, Threshold currents under pressure in InGaAsSb/AlGaAsSb laser diodes, Phys. Status Solidi B 244 (2007) 187–191.
[30] K.J. Cheetham, A. Krier, I.P. Marko, A. Aldukhayel, S.J. Sweeney, Direct evidence for suppression of Auger recombination in GaInAsSbP/InAs mid-infrared light-emitting diodes, Appl. Phys. Lett. 99 (2011) 141110.
[31] A. Rogalski, HgCdTe infrared detector material: history, status and outlook, Rep. Progr. Phys. 68 (2005) 2267–2336.
[32] N.L. Bazhenov, K.D. Mynbaev, V.I. Ivanov-Omski, V.A. Smirnov, V.P. Evtikhiev, N.A. Pikhtin, M.G. Rastegaeva, A.L. Stankevich, I.S. Tarasov, A.S. Shkol'nik, G.G. Zegrya, Temperature dependence of the threshold current of QW lasers, Semiconductors 39 (2005) 1210–1214.